Plant Science 231 (2015) 191–197

Contents lists available at ScienceDirect

Plant Science

journal homepage: www.elsevier.com/locate/plantsci

VvGONST-A and VvGONST-B are Golgi-localised GDP-sugar transporters in grapevine (*Vitis vinifera* L.)

Daniella Utz[a,b], Michael Handford[b,*]

[a] *Facultad de Ciencias Agronómicas, Universidad de Chile, Santiago, Chile*
[b] *Departamento de Biología, Facultad de Ciencias, Universidad de Chile, Santiago, Chile*

ARTICLE INFO

Article history:
Received 20 August 2014
Received in revised form
19 November 2014
Accepted 22 November 2014
Available online 6 December 2014

Keywords:
Cell wall
Glucomannan
Golgi apparatus
Nucleotide sugar transporter
Vitis vinifera

ABSTRACT

Plant nucleotide-sugar transporters (NSTs) are responsible for the import of nucleotide-sugar substrates into the Golgi lumen, for subsequent use in glycosylation reactions. NSTs are specific for either GDP- or UDP-sugars, and almost all transporters studied to date have been isolated from *Arabidopsis thaliana* L. In order to determine the conservation of the import mechanism in other higher plant species, here we report the identification and characterisation of VvGONST-A and VvGONST-B from grapevine (*Vitis vinifera* L. cv. Thompson Seedless), which are the orthologues of the GDP-sugar transporters GONST3 and GONST4 in *Arabidopsis*. Both grapevine NSTs possess the molecular features characteristic of GDP-sugar transporters, including a GDP-binding domain (GXL/VNK) towards the C-terminal. *VvGONST-A* and *VvGONST-B* expression is highest at berry setting and decreases throughout berry development and ripening. Moreover, we show using green fluorescent protein (GFP) tagged versions and brefeldin A treatments, that both are localised in the Golgi apparatus. Additionally, *in vitro* transport assays after expression of both NSTs in tobacco leaves indicate that VvGONST-A and VvGONST-B are capable of transporting GDP-mannose and GDP-glucose, respectively, but not a range of other UDP- and GDP-sugars. The possible functions of these NSTs in glucomannan synthesis and/or glycosylation of sphingolipids are discussed.

1. Introduction

In plants, the Golgi apparatus is responsible for the synthesis of non-cellulosic polysaccharides of the cell wall and also for the glycosylation of lipids and proteins. Lumenal glycosylation reactions are catalysed by enzymes called glycosyltransferases (GTs), which use sugars activated by the addition of a nucleotide. Most of the enzymes involved in the synthesis of nucleotide-sugars are cytoplasmic, although there is evidence of some interconversion within the lumen of the Golgi [1]. More recently, it has been reported that some Cellulose Synthase Like (CSL) GTs such as CSLA9 have their active site orientated towards the lumen of the Golgi apparatus [2]. CSLA9 synthesises glucomannan, requiring GDP-mannose and GDP-glucose as substrates [3], and it has been proposed that the CSLA family, composed of 9 members in *Arabidopsis thaliana* is responsible for the generation of this non-cellulosic polysaccharide in diverse plant species [4]. Therefore, considering the location of nucleotide-sugar synthesis in the cytosol, and their use as substrates by lumenal-facing enzymes, nucleotide-sugar transporters (NSTs) are required to transport the substrate across the membrane of the Golgi apparatus [5–8].

In plants, several NSTs have been identified and some have been cloned and characterised. UDP-galactose transporters (AtUTr2, AtNST-KT, UDPGalT1 and UDPGalT2 [9–11]), and transporters of UDP-galactose/UDP-glucose (AtUTr7 and OsUGT [12,13]) have been reported. In addition, in *Arabidopsis*, there is a family of NSTs termed GONST1-5 (Golgi Nucleotide Sugar Transporter; At2g13650, Atg07290, At1g76340, At5g19980, At1g21870, respectively [5,6]) that are orthologues of the GDP-mannose transporters VRG4 described in *Saccharomyces cerevisiae* [14], LPG2 from *Leishmania donovani* [15], CgVRG4 from *Candida glabrata* [16] and CaVRG4 from *C. albicans* [17].

NSTs are proteins which are typically approximately 350 amino acids in length, with molecular weights of around 35 kDa [8,18]. Moreover, they are highly hydrophobic, and computer-based algorithms predict that they harbour 6–10 transmembrane domains

Abbreviations: CSL, cellulose synthase-like; ER, endoplasmic reticulum; GDP, guanosine diphosphate; GFP, green fluorescent protein; GONST, Golgi Nucleotide Sugar Transporter; GTs, glycosyltransferases; NDP, nucleotide diphosphate; NSTs, nucleotide-sugar transporters; UDP, uridine diphosphate.

* Corresponding author at: Departamento de Biología, Facultad de Ciencias, Universidad de Chile, Las Palmeras 3425, Ñuñoa, Santiago, Chile. Tel.: +56 2 29787263; fax: +56 2 22712983.
E-mail addresses: dani.utz@gmail.com (D. Utz), mhandfor@uchile.cl (M. Handford).

http://dx.doi.org/10.1016/j.plantsci.2014.11.009
0168-9452/

(TMDs), consistent with their location embedded in a membrane. It has also been determined that the protein sequence of GONST1-4 and other GDP-sugar transporters [5,6,16,17] contain a conserved GX(L/V)NK motif, which in the case of VRG4 from *S. cerevisiae* has been shown to bind the guanosine diphosphate portion of GDP-sugars [19]. After the GDP-sugars have been used by lumenal facing GTs, GMP is produced by the action of an NDPase [8]. It has been postulated that an NK motif located towards the amino-terminal of these NSTs facilitates the export of the nucleoside-monophosphate, in exchange for the import of the GDP-sugar(s) [6].

Although the vast majority of the characterised plant NSTs has been identified in *Arabidopsis*, it has been proposed that the mechanism of delivery of nucleotide-sugars is conserved, given that other higher plant species also harbour NSTs in their genomes [8]. To date, this hypothesis has been tested for UDP-sugar transport [13], but not for GDP-sugar transport. However, it is not possible to predict the functions and subcellular localisation of possible NSTs based only on sequence similarities. For example, although many NSTs are closely related at the primary sequence level, their specificity of transport may differ [12]. In addition, not all NSTs are localised in the Golgi membrane; AtUTr1 and AtUTr3 are present in the ER where they are involved in the process of protein folding through the calnexin/calreticulin cycle [20,21]. Therefore, experimental functional characterisation of all predicted genes is necessary to determine their specificity and localisation *in planta*.

In this study, we report the cloning and characterisation of two NSTs from grapevine (*Vitis vinifera* L.). Grapevine is one of the most cultivated fruit crops in the world, and grape berries are commercialised as table grapes and dried fruits, and processed in wine making, with Chile being a leading producer and exporter of these products. Grape berries contain polysaccharides, and glycoproteins decorated with sugars which originate from GDP-sugars, implicating the necessity of NSTs for their import into the Golgi apparatus. We called these grapevine NSTs VvGONST-A and VvGONST-B, the most-closely related orthologues of GONST3 and GONST4, respectively. *VvGONST-A* and *VvGONST-B* are widely expressed throughout berry development, and by heterologous expression in tobacco leaves, we show that both NSTs are Golgi-localised and capable of transporting different GDP-sugars.

2. Materials and methods

2.1. Plant material

To characterise VvGONST-A and VvGONST-B, three grapevine plants (*V. vinifera* L. cv. Thompson Seedless) were selected from a field located in INIA La Platina (Chile), during the 2012 growing season. Samples for RNA extraction were frozen in liquid nitrogen and stored at −80 °C.

2.2. Cloning of VvGONST-A and VvGONST-B and vector construction

The nucleotide sequences of *A. thaliana GONST3* and *GONST4* (accession numbers At1g76340 and At5g19980, respectively) were used in a tBLASTn search to identify orthologous gene models in the Grape Genome Browser (version 12X) designed by Genoscope (the French National Sequencing Center; http://www.genoscope.cns.fr/vitis).

VvGONST-A and *VvGONST-B* cDNA were amplified from *V. vinifera* cv. Thompson Seedless leaf cDNA using *Pfu* polymerase (Fermentas) and primers VvGONST-A-F (5′-ATGTCTAATG ATGAGGAGAATC-3′) and VvGONST-A-R (5′-TTTCCCCTCTTGTG-AATT-3′), and VvGONST-B-F (5′-ATGTCTTCGACTAGATTTGATT-3′) and VvGONST-B-R (5′-TACTGC AGCAAGTTTACCC-3′). Both primers flank the coding region and the PCR product was cloned into pCR8 (Invitrogen) forming pCR8-VvGONST-A and pCR8-VvGONST-B and then homologously recombined into the Gateway-compatible vector, pGWB5 for the addition of a C-terminal GFP tag [22].

2.3. Computational analysis

Protein sequences were aligned using Clustal-OMEGA. The phylogenetic analysis was carried out using the Mega 6.06 software package [23]. Hydrophobicity analysis was performed using a Kyte-Doolittle hydrophobicity plot. The number of putative TMDs was estimated using the web-based algorithms TMHMM, SOSUI, TOPRED, HMMTOP and PRODIV-TMHMM.

2.4. RNA isolation and quantitative expression analysis of VvGONST-A and VvGONST-B in V. vinifera

Total RNA from berry stages E-L27, 29, 30, 31, 35 and 38 [24], and mature leaves was isolated as described by Reid et al. [25]. RNA concentration and integrity were measured after DNase I (Fermentas) treatment with a NanoDrop3300 Fluorospectrometer (ThermoScientific) and agarose gel electrophoresis under denaturing conditions. By use of a common oligo AP primer (5′-CGCCACGCGTCGACTAGTACTTTTTTTTTTTTTTTT-3′), 0.5 μg of DNAse I-treated total RNA were heated (70 °C, 5 min) and then subjected to a reverse transcription (RT) reaction using Improm-II reagents (Promega). Quantitative polymerase chain reactions (qPCR) were performed with an Mx3000P Real-Time PCR System (Stratagene), using the SensiMix SYBRkit (Bioline) to monitor dsDNA synthesis. The following standard thermal profile was used for two-step cycling qPCR reactions: 95 °C for 10 min and 40 cycles of 95 °C for 15 s, 58 °C for 1 min. No-template controls were included for each primer pair and each PCR reaction was performed in triplicate. Dissociation curves for each amplicon were then analysed to verify the specificity of each amplification reaction; the dissociation curve was obtained by heating the amplicon from 60 °C to 95 °C. Data were analysed using MxPro system software (Stratagene). The expression of three reference genes, *Actin* (Genbank accession: EC969944), *EF1-α* (Genbank accession: EC959059) and *GAPDH* (Genbank accession: ECCB973647) [25] was monitored and *GAPDH* was selected using NormFinder [26]. *VvGONST-A* and *VvGONST-B* transcript levels were normalised to the expression of *GAPDH* using the ΔCt method [27]. The sequences of the primer pairs used were: *VvGONST-A* (5′-TTTGTGGGGACAGTTGGGCT TTT-3′ and 5′-CTCTCTTGCACTTTCACGTCCGTT-3′), *VvGONST-B* (5′-AGGAAGGCAATC TCTGCCAC-3′ and 5′-AGGAGGCAAACCAA-CCCAAA-3′), *Actin* (5′-CTTGCATCCCTCAG CACCTT-3′ and 5′-TCCTGTGGACAATGGATGGA-3′), *EF1-α* (5′-GAACTGGGTGCTTGA TAGGC-3′ and 5′-AACCAAAATATCCGGAGTAAAAGA-3′) and *GAPDH* (5′-TTCTCGTTG AGGGCTATTCCA-3′ and 5′-CCACAGACTTCATCGG-TGACA-3′). All qPCR data represent the average of three biological pools of samples and three technical replicates. *In silico* analyses were performed using data provided in www.plexdb.org.

2.5. Subcellular localisation of VvGONST-A and VvGONST-B

Leaves of tobacco (*Nicotiana tabacum*) were used for transient expression after *Agrobacterium tumefaciens*-mediated transformation (strain GV3101) with pGWB5-VvGONST-A-GFP or pGWB5-VvGONST-B-GFP by syringe infiltration as described by previously [28]. Lower epidermal peels of transformed leaves were analysed 4 d after infiltration with a bacterial culture ($OD_{600\,nm}$ 0.5–0.7). In some cases, samples were incubated in 100 μg mL^{-1} Brefeldin A solution for 2 h. Some samples were agroinfiltrated using the Golgi marker (G-rk CD3-967) or the ER marker (ER-rk CD3-959) [29]. Images were captured with a confocal microscope (LSM510 Meta

or LSM710 Carl Zeiss) and processed with ImageJ 1.45s. Overlap coefficients were calculated using Zeiss ZEN 2012 software.

2.6. Tobacco leaf transformation, subcellular fractionation, and nucleotide-sugar uptake assays of VvGONST-A and VvGONST-B

Tobacco leaves were agro-infiltrated with pGWB5, pGWB5-VvGONST-A-GFP, pGWB5–VvGONST-B–GFP. After 4 d, accumulation of VvGONST-A-GFP and VvGONST-B-GFP was determined by epifluorescence microscopy (Olympus IX70), samples were processed as described by Norambuena [9], and then immunoblotted using a monoclonal anti-GFP antiserum (Sigma). Subsequently, protein concentrations in the Golgi-enriched vesicle fractions were determined by the Bradford method and 40–50 μg used in filter-based uptake assays with a panel of commercially available radiolabeled nucleotide-sugars: GDP-[^{3}H]fucose (16 Ci/mmol) (Perkin-Elmer), GDP-[^{14}C]glucose (300 mCi/mmol) (American Radiolabeled Chemicals Inc.), GDP-[^{14}C]mannose (262 mCi/mmol) (Perkin-Elmer) and UDP-[^{3}H]glucose (3.5 Ci/mmol) (GE Healthcare).

3. Results and discussion

3.1. Protein sequence analysis of VvGONST-A and VvGONST-B

To identify candidate orthologous sequences of GONST3 (At1g76340) and GONST4 (At5g19980) of *Arabidopsis* in the reference genome PN40024 from *V. vinifera* [30], a bioinformatics search was performed using tBLASTn. Two protein sequences with 81% and 78% identity, respectively were selected. We designated these grapevine sequences VvGONST-A (Genbank accession: XP_002271444.1) and VvGONST-B (Genbank accession: XP_002284977.1).

VvGONST-A and *VvGONST-B* were cloned from Thompson Seedless cDNA, and comparisons with their respective genomic sequences highlight the absence of introns in both cases, as also found for their *Arabidopsis* orthologues, *GONST3* and *GONST4* [6]. The nucleotide sequences cloned from Thompson Seedless were 99.5% and 99.7% identical with respect to the reference genome PN40024, translating into two and one amino acid substitutions, respectively (Fig. 1A and B). *VvGONST-A* is located on chromosome 10, whereas *VvGONST-B* is on chromosome 11. At the protein level, VvGONST-A has 374 amino acids with a calculated molecular mass of 41.8 kDa and VvGONST-B has 349 amino acids with a calculated molecular mass of 37.8 kDa. The predicted isoelectric points of VvGONST-A and VvGONST-B are 4.9 and 7.7, respectively, identical to those of GONST3 and GONST4 from *Arabidopsis* [6]. It has been predicted that both *Arabidopsis* orthologues have 10 TMDs [6]. We predicted the topology of VvGONST-A and VvGONST-B by using Kyte-Doolittle hydrophobicity plots. As a result, both highly hydrophobic grapevine proteins are also predicted to harbour 10 TMDs (Fig. 1A and B). Many plant NSTs are predicted to possess an even number of TMDs [8], and the membrane topology of several of these transporters has been predicted *in silico* [13,31]. Using the TOPCONS algorithm (http://topcons.cbr.su.se/; [32]), the predicted topology of both VvGONST-A and VvGONST-B places the N- and C-termini facing the cytosol. In addition, both NSTs contain a conserved GDP-binding motif GX(L/V)NK (VvGONST-A, GIVNK; VvGONST-B, GVVNK) located between TMDs VIII and IX, and both present in their sequence the putative GMP-binding NK domain between TMDs I and II (Fig. 1A and B). The predicted membrane topologies of these NSTs locates the GX(L/V)NK and NK motifs in the cytosol and lumen, respectively, consistent with their proposed roles in GDP-sugar import and GMP export.

Using NST sequences of plants and other species, we constructed an unrooted phylogenetic tree of VvGONST-A and VvGONST-B using Clustal-OMEGA and Mega 6.06. Phylogenetic analysis shows that VvGONST-A is in the same clade as GONST3 and VvGONST-B is in the same clade as GONST4. Moreover, GDP-mannose transporters, including GONST1, VRG4 and LPG2 group in a different, but nearby clade, whereas UDP-sugar transporters are more distantly related (Fig. 2). Taken together, these molecular and phylogenetic characteristics are consistent with VvGONST-A and VvGONST-B being GDP-sugar transporting NSTs.

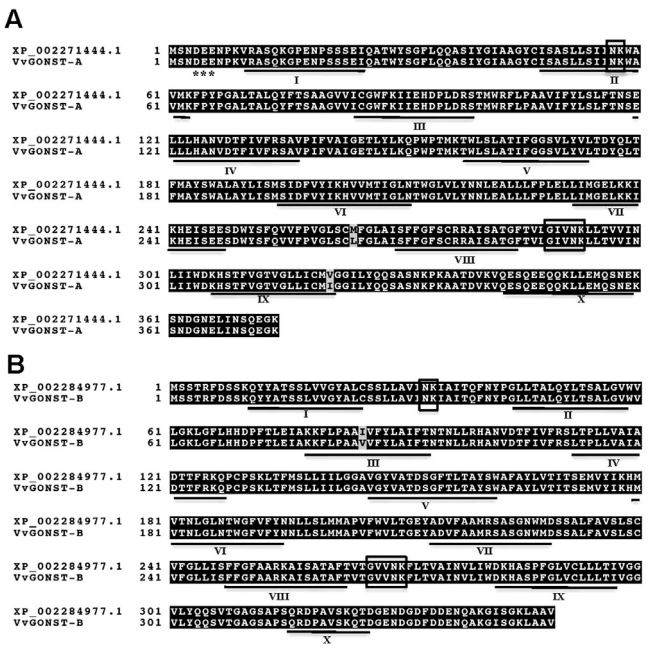

Fig. 1. Sequence analysis of grapevine VvGONST-A and VvGONST-B. (A) Alignment of VvGONST-A from Thompson Seedless with XP_002271444.1 from the reference genome PN40024. (B) Alignment of VvGONST-B from Thompson Seedless with XP_002284977.1 from the reference genome PN40024. Sequence alignments were performed using Clustal-OMEGA. Black and grey shading indicate identical and conservative amino acid substitutions, respectively. The predicted transmembrane domains are underlined (I–X). The locations of conserved motifs involved in substrate transport are boxed. Asterisks denote a Golgi-targetting motif in VvGONST-A.

3.2. Expression analysis of VvGONST-A and VvGONST-B

In order to determine the expression profile of *VvGONST-A* and *VvGONST-B* throughout berry development, we carried out quantitative RT-PCR analysis using RNA extracted from berry stages E-L27 to 38. Stages E-L27 to E-L33 represent the formation of berries, from setting to being hard and green, whilst E-L34 to E-L38 covers berry ripening until harvesting [24].

Of the three reference genes tested (*Actin*, *EF1-α* and *GAPDH*), *GAPDH* has the greatest stability of expression in the different stages analysed. Therefore, this gene was used to normalise transcript levels of both NSTs at the stages sampled. Our findings show that *VvGONST-A* and *VvGONST-B* transcripts were not confined to berries, and were not constant during berry development. Specifically, the expression of *VvGONST-A* was highest at the E-L27 stage (berry setting: young berries enlarging (>2 mm diameter), bunch at right angles to stem [24]) and then fell significantly by approximately 67% at the harvest ripe stage, E-L38 (Fig. 3A). *VvGONST-B* expression was also highest in E-L27 stage berries and suffered a 74% reduction by E-L38 (Fig. 3B). As comparisons, transcript levels of both NSTs in mature leaves were similar to those found during the mid-stages of berry development. Globally, transcript levels of *VvGONST-B* were approximately 40-times greater than those of *VvGONST-A* at all stages of berry development analysed, which

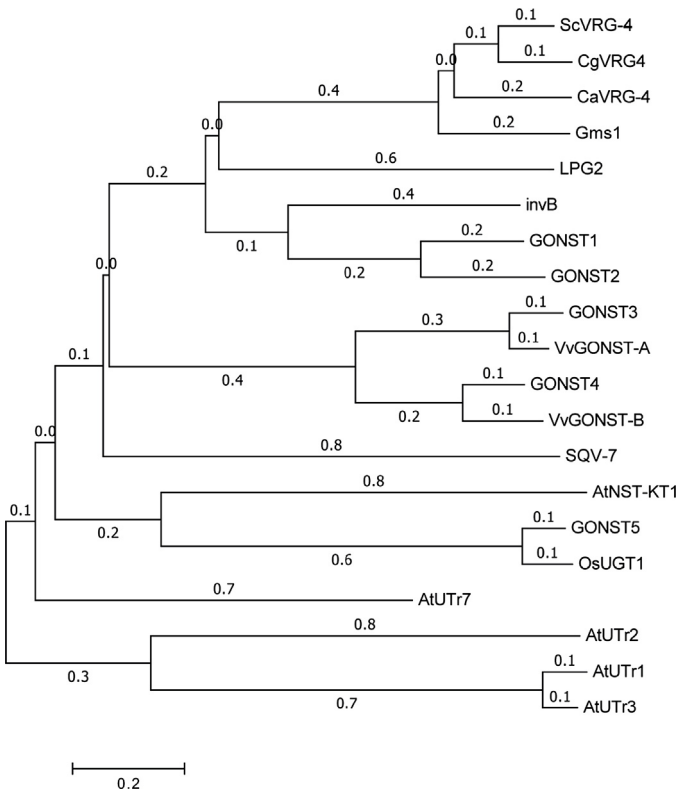

Fig. 2. Phylogenetic analysis of VvGONST-A and VvGONST-B. The unrooted tree was constructed using MUSCLE and the phylogenetic analysis was performed with the Neighbour-Joining method. The tree is drawn to scale, with branch lengths in the same units as those of the evolutionary distances used to infer the phylogenetic tree. The 0.2 scale bar represents 0.2-amino acid substitutions per site. The accession numbers of each sequence used to construct the tree are shown in Supplementary Table A.1.

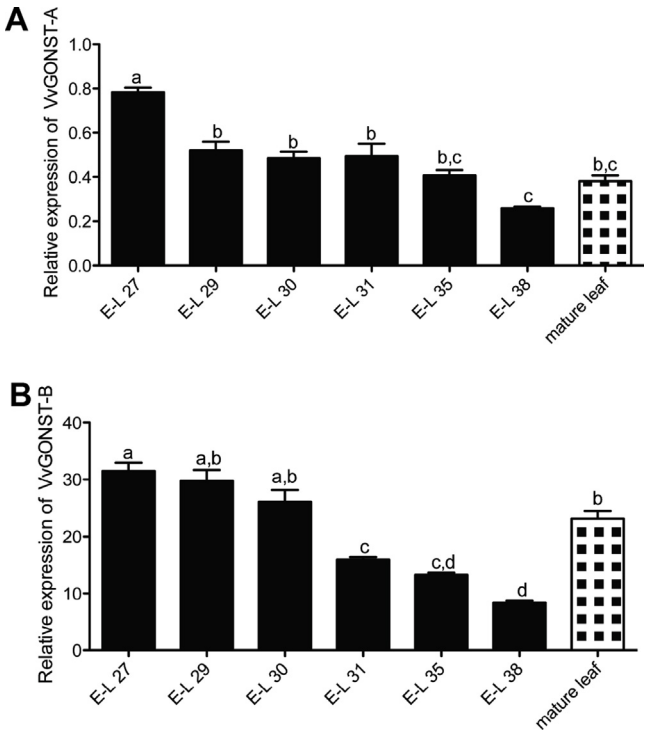

Fig. 3. Expression analysis of *VvGONST-A* and *VvGONST-B*. Transcript levels of *VvGONST-A* (A) and *VvGONST-B* (B) were determined by qRT-PCR in berry stages E-L27, 29, 30, 31, 35 and 38, and in leaves of field-grown Thompson Seedless grapevines. The data were normalised using *GAPDH* as a control. Different letters indicate significant differences between values, as determined by means of one-way ANOVA and a Bonferroni post-test ($p < 0.05$). SE bars are shown ($n = 3$).

could be related to the transport functions of the corresponding proteins.

The expression profile of both NSTs was also queried bioinformatically using the GeneChip 16K Microarray PLEXdb database (http://www.plexdb.org/) for *VvGONST-B*. According to the experiment identified as "VV11: Pinot Noir berry transcriptome during ripening" (Stefania Pilati, the IASMA Research Center – Italy), the expression of *VvGONST-B* (as represented by the closely related Gene ID, 1611331_at) fell consistently in each of three seasons between stages E-L33 and E-L36 in Pinot Noir berries, a finding which was also observed in both grape flesh and grape skins of Muscat Hamburg table grapes ["VV33: Grape flesh and skin ripening transcriptomic profiling", Pablo Carbonell-Bejerano, Instituto de las Ciencias de la Vid y el Vino, Spain; Gene ID VVTU2092_at, GrapeGen (Custom Affymetrix Grape) Array]. Both *in silico* analyses are thus concordant with our experimental results (Fig. 3B). In addition, saline and osmotic stress resulted in a 10-fold reduction in *VvGONST-B* expression in leaves of Cabernet Sauvignon plants exposed to these conditions for 24 h ("VV1: short term abiotic stress Cabernet Sauvignon", Elizabeth Tattersall, University of Nevada). No Gene IDs closely related to *VvGONST-A* are present on the GeneChip 16K, which represents approximately 50% of *V. vinifera* gene sequences, impeding similar experimental and *in silico* comparisons for this NST.

3.3. Subcellular localisation of VvGONST-A and VvGONST-B

Computer-based analyses of the VvGONST-A and VvGONST-B amino acid sequences predict that both proteins could be located in the plasma membrane or in the Golgi apparatus (http://psort.hgc.jp/; data not shown). Considering that no known reactions require the presence of NSTs at the plasma membrane, and that VvGONST-A harbours a diacidic motif (DEE) at its amino terminus, which has been implicated in the export of Golgi-localised membrane proteins from the ER in plants [33], we consider from the bioinformatic analysis that an organellar localisation is more probable. One of the functions of the Golgi apparatus is the glycosylation of macromolecules, and it has been shown in *Arabidopsis* that many NSTs are localised in this organelle [5–7,9,12], consistent with their role in the transport of substrates required for glycosylation reactions. However, some NSTs are located in the ER [20,21]. Therefore, the subcellular localisation of VvGONST-A and VvGONST-B was determined experimentally, by fusing GFP in frame to the C-terminus of both NSTs. VvGONST-A-GFP and VvGONST-B-GFP were then transiently expressed by *Agrobacterium*-mediated infiltration of tobacco leaves.

Four days after infiltration, spots of green fluorescence were observed, of approximately 1 μm in diameter in the case of both grapevine NSTs (Fig. 4A and D). The overlap coefficients in samples coinfiltrated with the NSTs and a known Golgi marker, G-rk CD3-967 [29] were 86% and 88%, for VvGONST-A-GFP/G-rk CD3-967 and VvGONST-B-GFP/G-rk CD3-967, respectively (Fig. 4C and F). The fluorescence patterns did not have the same distributions as that of an ER marker (ER-rk CD3-959) composed of a red fluorescent protein fused at its N-terminus to the signal peptide of AtWAK2, and at its C-terminus to a known ER retention signal [29] (Fig. 4G–J). Overlap coefficients between the NSTs and the ER marker were <50%.

To further analyse the subcellular localisation of VvGONST-A and VvGONST-B, the epidermal cells were visualised after pretreatment with Brefeldin A (BFA), a drug known to alter the distribution of Golgi proteins to the ER in leaves [34]. Treatment with this drug dramatically altered the pattern of protein localisation of both NSTs,

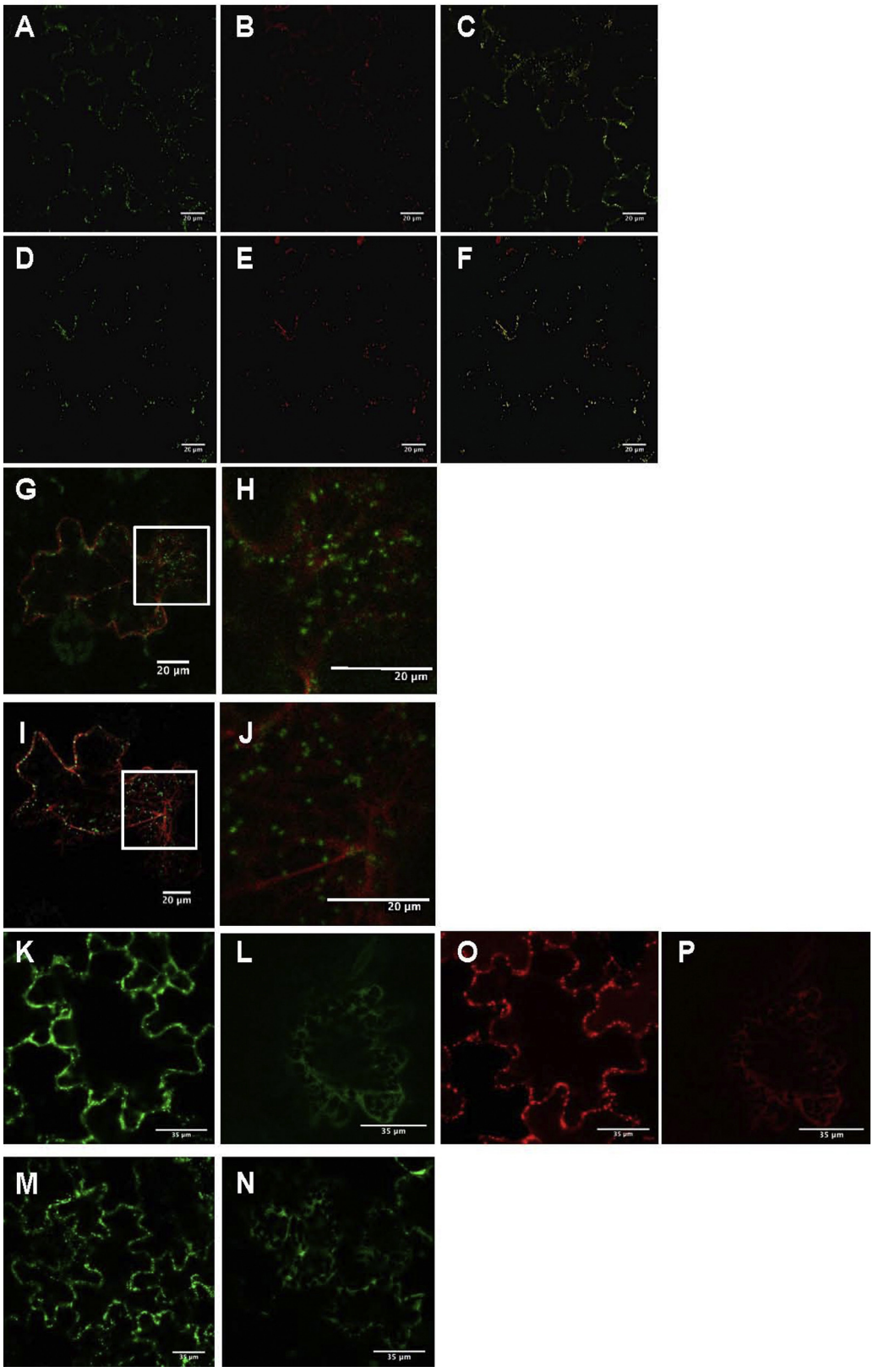

Fig. 4. Subcellular distribution of VvGONST-A and VvGONST-B. GFP-fusion versions of VvGONST-A and VvGONST-B were transformed into tobacco leaves by *Agrobacterium*-mediated syringe infiltration. Samples were observed by confocal microscopy 4 d after infiltration. (A and D) Distribution of VvGONST-A-GFP and VvGONST-B, respectively. (B and E) Distribution of Golgi marker (G-rk CD3-967). (C) Merge of (A) and (B). (F) Merge of (D) and (E). (G) Merge of VvGONST-A-GFP and the ER marker, ER-rk CD3-959. (H) Zoom of box in (G). (I) Merge of VvGONST-B-GFP and the ER marker, ER-rk CD3-959. (J) Zoom of box in (I). (K, M and O) Distribution of VvGONST-A-GFP, VvGONST-B-GFP and Golgi marker (G-rk CD3-967) prior to Brefeldin-A treatment, respectively. (L, N and P) Distribution of VvGONST-A-GFP, VvGONST-B-GFP and Golgi marker (G-rk CD3-967) in cells incubated with 100 $\mu g\,mL^{-1}$ Brefeldin-A for 2 h, respectively. *Note*: cells co-infiltrated with VvGONST-A-GFP and Golgi marker (G-rk CD3-967) are shown in images (K) and (O), and (L) and (P).

resulting in a mesh-like pattern of fluorescence, resembling the ER network (Fig. 4K–N) and similar to that found when a known Golgi marker, α-1,2-mannosidase I was subjected to the same treatment (G-rk CD3-967; Fig. 4O and P) [29]. In addition, prior to the addition of BFA, the fluorescent spots in VvGONST-A-GFP- and VvGONST-B-GFP-infiltrated leaves were highly motile (Supplementary Videos A.1–A.4). Taken together, we conclude from the size, motility, and sensitivity to BFA that VvGONST-A-GFP and VvGONST-B-GFP are Golgi-localised proteins, and confirm that the absence of diacidic motifs in VvGONST-B does not exclude the possibility that proteins are found in this organelle [33].

3.4. Substrate specificity of VvGONST-A and VvGONST-B

Based exclusively on sequence similarity, it is not possible to predict the substrate specificity of VvGONST-A and VvGONST-B. Therefore, we performed transport assays for VvGONST-A and VvGONST-B using Golgi-enriched vesicles extracted from tobacco leaves previously transformed with VvGONST-A-GFP, VvGONST-B-GFP and with pGWB5 alone as a control. The transformation was confirmed by checking NST-infiltrated samples for GFP fluorescence by epifluorescence microscopy, just prior to extraction of the Golgi-enriched vesicles by subcellular fractionation. In addition, accumulation of both tagged-NSTs in the Golgi-enriched fractions was confirmed by immunoblot analysis using an anti-GFP antiserum (Supplementary Figure A.1).

The Golgi-enriched vesicles containing equal amounts of protein obtained from control, VvGONST-A-GFP and VvGONST-B-GFP infiltrated samples were used in assays to measure the uptake of a panel of commercially available radiolabeled NDP-sugars. This panel was comprised of GDP-mannose, GDP-fucose, GDP-glucose and UDP-glucose, the latter used to confirm whether the presence of the GDP-binding motif, GX(L/V)NK, precludes the uptake of a sugar bound to a different nucleotide.

We determined that the uptake of GDP-mannose was higher in vesicles isolated from tobacco expressing VvGONST-A-GFP than in the control (Fig. 5A). Experiments with GDP-glucose, GDP-fucose or UDP-glucose revealed no significant uptake of these nucleotide-sugars by VvGONST-A-GFP. On the other hand, we determined that VvGONST-B-GFP is capable of transporting GDP-glucose, but not the other GDP- or UDP-sugars in the panel tested (Fig. 5B). We conclude from these findings that the requirement for GDP-sugar import is conserved in higher plant species other than *Arabidopsis*, as well as in green algae (*Volvox carteri* [35]).

What are the potential uses of GDP-mannose and GDP-glucose inside the Golgi lumen? Recently, it has been shown that the active site of CSLA9 in *Arabidopsis* faces the lumen of this organelle [2]. This enzyme is responsible for glucomannan synthesis in this species, together with other members of the CSLA family [3,36]. Glucomannan synthesis requires both GDP-mannose and GDP-glucose, so VvGONST-A and VvGONST-B may be involved in transporting these substrates into the Golgi lumen. We believe this to be a strong possibility, given the presence of glucomannan in the cell walls of many plant species, including fruits and gymnosperms [37,38]. On searching the reference genome, we found a potential AtCSLA9 orthologue in grapevine (Genbank accession: XM_002283636.2 [39]). On performing hydrophobicity analysis of this orthologue, we predict that it also harbours five TMDs and that its active site is oriented towards the lumen, concordant with the need for NSTs, including VvGONST-A and VvGONST-B for the import of these substrates.

Nevertheless, the GDP-mannose imported by VvGONST-A may also be diverted towards glycolipid decoration. Recently, it has been shown that *Arabidopsis* mutants in the GDP-mannose transporter, GONST1, have significantly less mannosylation of glycosphingolipids [40]. Although to our knowledge, there are no studies on

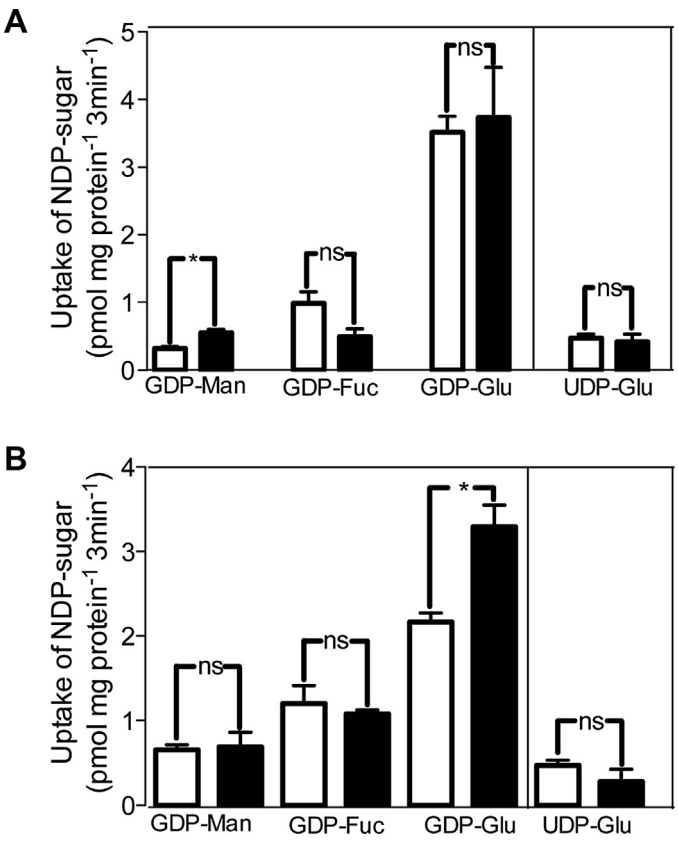

Fig. 5. Substrate specificity of VvGONST-A and VvGONST-B expressed in tobacco cells. The substrate specificity of VvGONST-A-GFP (A) and VvGONST-B-GFP (B) was determined. Nucleotide-sugar uptake was determined in microsomal vesicles isolated from tobacco leaves infiltrated with vector without insert (white bars) and VvGONST-A-GFP or VvGONST-B-GFP (black bars). Microsomal vesicles were incubated for 3 min at 25 °C with radiolabelled nucleotide-sugar (1 μM, 0.1 μCi) and reactions were stopped by filtration. The averages of a representative assay with SE bars are shown ($n = 3$). Data were analysed by a Student's *t*-test (*, $p < 0.05$; ns, not significant).

the presence of mannosphingolipids in grape berries, VvGONST-A could also be involved in importing the substrate for use by mannosyltransferases responsible for decoration of equivalent glycolipids in this species.

VvCSTLP1, an NST related to CMP-sialic acid transporters, has recently been identified in *V. vinifera*. Nevertheless, it possesses both N- and C-terminal ER retention signals and it is uncertain whether VvCSTLP1 functions as a true CMP-sialic acid transporter [31]. With the identification and characterisation of VvGONST-A and VvGONST-B, our results lead us to conclude that one of the steps of the glycosylation process, that of substrate import into the Golgi lumen, is indeed conserved in this species. The generation and phenotypic analysis of grapevine plants lacking one or both of these NSTs would provide compelling evidence for the precise function performed by these proteins in *V. vinifera*.

Acknowledgements

We wish to thank Dr Manuel Pinto (INIA, La Platina/CEAF), Dr Ariel Orellana (UNAB), Lorena Saragoni, Alexis Vergara, Cecilia Rodríguez-Furlán, Claudia Clavero and Javier Campos for technical assistance and for supplying grapevine samples. We gratefully acknowledge funding from Beca Conicyt (21090418 and 24120980; D.U.), Fondecyt 1106040, 1100129 and 1140527, and PBCT Anillo ACT-1110 (to M.H.) and the Doctorado en Ciencias Silvoagropecuarias y Veterinarias programme of the Universidad de Chile (to D.U.).

Appendix A. Supplementary data

Supplementary data associated with this article can be found, in the online version, at http://dx.doi.org/10.1016/j.plantsci.2014.11.009.

References

[1] M. Bar-Peled, M.A. O'Neill, Plant nucleotide sugar formation, interconversion, and salvage by sugar recycling, Annu. Rev. Plant Biol. 62 (2011) 127–155.
[2] J. Davis, F. Brandizzi, A.H. Liepman, K. Keegstra, Arabidopsis mannan synthase CSLA9 and glucan synthase CSLC4 have opposite orientations in the Golgi membrane, Plant J. 64 (2010) 1028–1037.
[3] F. Goubet, C.J. Barton, J.C. Mortimer, X. Yu, Z. Zhang, G.P. Miles, J. Richens, A.H. Liepman, K. Seffen, P. Dupree, Cell wall glucomannan in Arabidopsis is synthesized by CSLA glycosyltransferases, and influences the progression of embryogenesis, Plant J. 60 (2009) 527–538.
[4] A.H. Liepman, C.J. Nairn, W.G. Willats, I. Sørensen, A.W. Roberts, K. Keegstra, Functional genomic analysis supports conservation of function among cellulose synthase-like a gene family members and suggests diverse roles of mannans in plants, Plant Physiol. 143 (2007) 1881–1893.
[5] T.C. Baldwin, M.G. Handford, M.I. Yuseff, A. Orellana, P. Dupree, Identification and characterization of GONST1, a Golgi-localized GDP-mannose transporter in *Arabidopsis*, Plant Cell 13 (2001) 2283–2295.
[6] M.G. Handford, F. Sicilia, F. Brandizzi, J.H. Chung, *Arabidopsis thaliana* expresses multiple Golgi-localised nucleotide-sugar transporters related to GONST1, Mol. Genet. Genomics 272 (2004) 397–410.
[7] L. Norambuena, L. Marchant, P. Berninsone, C.B. Hirschberg, H. Silva, A. Orellana, Transport of UDP-galactose in plants. Identification and functional characterization of AtUTr1, an *Arabidopsis thaliana* UDP-galactose/UDP-glucose transporter, J. Biol. Chem. 277 (2002) 32923–32929.
[8] F. Reyes, A. Orellana, Golgi transporters: opening the gate to cell wall polysaccharide biosynthesis, Curr. Opin. Plant Biol. 11 (2008) 244–251.
[9] L. Norambuena, R. Nilo, M. Handford, F. Reyes, L. Marchant, L. Meisel, A. Orellana, AtUTr2 is an *Arabidopsis thaliana* nucleotide sugar transporter located in the Golgi apparatus capable of transporting UDP-galactose, Planta 222 (2005) 521–529.
[10] I. Rollwitz, M. Santaella, D. Hille, U. Flügge, K. Fischer, Characterization of AtNST-KT1, a novel UDP-galactose transporter from *Arabidopsis thaliana*, FEBS Lett. 580 (2006) 4246–4251.
[11] H. Bakker, F. Routier, S. Oelmann, W. Jordi, A. Lommen, R. Gerardy-Schahn, D. Bosch, Molecular cloning of two *Arabidopsis* UDP-galactose transporters by complementation of a deficient Chinese hamster ovary cell line, Glycobiology 15 (2005) 193–201.
[12] M. Handford, C. Rodríguez-Furlán, L. Marchant, M. Segura, D. Gómez, E. Álvarez-Buylla, G. Xiong, M. Pauly, A. Orellana, *Arabidopsis thaliana* AtUTr7 encodes a Golgi-localized UDP-Glucose/UDP-Galactose transporter that affects lateral root emergence, Mol. Plant. 5 (2012) 1263–1280.
[13] J. Seino, K. Ishii, T. Nakano, N. Ishida, M. Tsujimoto, Y. Hashimoto, S. Takashima, Characterization of rice nucleotide sugar transporters capable of transporting UDP-galactose and UDP-glucose, J. Biochem. 148 (2010) 35–46.
[14] N. Dean, Y.B. Zhang, J.B. Porter, The *VRG4* gene is required for GDP-mannose transport into the lumen of the Golgi in the yeast, *Saccharomyces cerevisiae*, J. Biol. Chem. 272 (1997) 31908–31914.
[15] D. Ma, D.G. Russell, S.M. Beverley, S.J. Turco, Golgi GDP-mannose uptake requires Leishmania LPG2. A member of a eukaryotic family of putative nucleotide-sugar transporters, J. Biol. Chem. 272 (1997) 3799–3805.
[16] A. Nishikawa, B. Mendez, Y. Jigami, N. Dean, Identification of a *Candida glabrata* homologue of the *S. cerevisiae* VRG4 gene, encoding the Golgi GDP-mannose transporter, Yeast 19 (2002) 691–698.
[17] A. Nishikawa, J.B. Poster, Y. Jigami, N. Dean, Molecular and phenotypic analysis of *CaVRG4*, encoding an essential Golgi apparatus GDP-mannose transporter, J. Bacteriol. 184 (2002) 29–42.
[18] M. Handford, C. Rodriguez-Furlán, A. Orellana, Nucleotide-sugar transporters: structure, function and roles *in vivo*, Braz. J. Med. Biol. Res. 39 (2006) 1149–1158.
[19] X. Gao, A. Nishikawa, N. Dean, Identification of a conserved motif in the yeast Golgi GDP-mannose transporter required for binding to nucleotide sugar, J. Biol. Chem. 276 (2001) 4424–4432.
[20] F. Reyes, L. Marchant, L. Norambuena, R. Nilo, H. Silva, A. Orellana, AtUtr1, a UDP-glucose/UDP-galactose transporter from *Arabidopsis thaliana*, is located in the endoplasmic reticulum and up-regulated by the unfolded protein response, J. Biol. Chem. 281 (2006) 9145–9151.
[21] F. Reyes, G. León, M. Donoso, F. Brandizzi, A.P.M. Weber, A. Orellana, The nucleotide sugar transporters AtUtr1 and AtUtr3 are required for the incorporation of UDP-glucose into the endoplasmic reticulum, are essential for pollen development and are needed for embryo sac progress in *Arabidopsis thaliana*, Plant J. 61 (2010) 423–435.
[22] T. Nakagawa, T. Kurose, T. Hino, K. Tanaka, M. Kawamukai, Y. Niwa, K. Toyooka, K. Matsuoka, T. Jinbo, T. Kimura, Development of series of gateway binary vectors, pGWBs, for realizing efficient construction of fusion genes for plant transformation, J. Biosci. Bioeng. 104 (2007) 34–41.
[23] K. Tamura, G. Stecher, D. Peterson, A. Filipski, S. Kumar, MEGA6. Molecular evolutionary genetics analysis version 6.0, Mol. Biol. Evol. 30 (2013) 2725–2729.
[24] B.G. Coombe, Adoption of a system for identifying grapevine growth stages, Aust. J. Grape Wine Res. 1 (1995) 100–110.
[25] K.E. Reid, N. Olsson, J. Schlosser, F. Peng, S.T. Lund, An optimized grapevine RNA isolation procedure and statistical determination of reference genes for real-time RT-PCR during berry development, BMC Plant Biol. 6 (2006) 27.
[26] C.L. Andersen, J.L. Jensen, T.F. Orntoft, Normalization of real-time quantitative reverse transcription-PCR data: a model-based variance estimation approach to identify genes suited for normalization, applied to bladder and colon cancer data sets, Cancer Res. 64 (2004) 5245–5250.
[27] M.W. Pfaffl, A new mathematical model for relative quantification in real-time RT-PCR, Nucleic Acids Res. 29 (2001) e45.
[28] M.F. Aguayo, D. Ampuero, P. Mandujano, R. Parada, R. Muñoz, M. Gallart, T. Altabella, R. Cabrera, C. Stange, M. Handford, SORBITOL DEHYDROGENASE is a cytosolic protein required for sorbitol metabolism in *Arabidopsis thaliana*, Plant Sci. 205–206 (2013) 63–75.
[29] B.K. Nelson, X. Cai, A. Nebenführ, A multicolored set of *in vivo* organelle markers for co-localization studies in *Arabidopsis* and other plants, Plant J. 51 (2007) 1126–1136.
[30] O. Jaillon, J. Aury, B. Noel, A. Policriti, C. Clepet, A. Casagrande, N. Choisne, S. Aubourg, N. Vitulo, C. Jubin, A. Vezzi, F. Legeai, F. Hugueney, C. Dasilva, D. Horner, E. Mica, D. Jublot, J. Poulain, C. Bruyère, A. Billault, B. Segurens, M. Gouyvenoux, E. Ugarte, F. Cattonaro, V. Anthouard, V. Vico, C. Del Fabbro, M. Alaux, G. Di Gaspero, V. Dumas, N. Felice, S. Paillard, I. Juman, M. Moroldo, S. Scalabrin, A. Canaguier, I. Le Clainche, G. Malacrida, E. Durand, G. Pesole, V. Laucou, P. Chatelet, D. Merdinoglu, M. Delledonne, M. Pezzotti, A. Lecharny, C. Scarpelli, F. Artiguenave, M.E. Pè, G. Valle, M. Morgante, M. Caboche, A. Adam-Blondon, J. Weissenbach, F. Quétier, P. Wincker, The grapevine genome sequence suggests ancestral hexaploidization in major angiosperm phyla, Nature 449 (2007) 463–467.
[31] B. Cakir, A.C. Olcay, Molecular cloning, phylogenetic analysis, and expression profiling of a grape CMP-sialic acid transporter-like gene induced by phytohormone and abiotic stress, Genes Genom 35 (2013) 225–238.
[32] A. Bernsel, H. Viklund, A. Hennerdal, A. Elofsson, TOPCONS: consensus prediction of membrane protein topology, Nucleic Acids Res. 37 (2009) W465–W468.
[33] S.L. Hanton, L. Renna, L.E. Bortolotti, L. Chatre, G. Stefano, F. Brandizzi, Diacidic motifs influence the export of transmembrane proteins from the endoplasmatic reticulum in plants cells, Plant Cell 17 (2005) 3081–3093.
[34] A. Nebenführ, C. Ritzenthaler, D. Robinson, A. Brefeldin, Deciphering an enigmatic inhibitor of secretion, Plant Physiol. 130 (2002) 1102–1108.
[35] N. Ueki, I. Nishii, Controlled enlargement of the glycoprotein vesicle surrounding a *Volvox* embryo requires the InvB nucleotide-sugar transporter and is required for normal morphogenesis, Plant Cell 21 (2009) 1166–1181.
[36] A.H. Liepman, C.G. Wilkerson, K. Keegstra, Expression of cellulose synthase-like (*Csl*) genes in insect cells reveals that *CslA* family members encode mannan synthases, Proc. Natl. Acad. Sci. U.S.A. 102 (2005) 2221–2226.
[37] D. Galvez-Lopez, F. Laurens, B. Quéméner, M. Lahaye, Variability of cell wall polysaccharides composition and hemicellulose enzymatic profile in an apple progeny, Int. J. Biol. Macromol. 49 (2011) 1104–1109.
[38] Y. Maeda, T. Awano, K. Takabe, M. Fujita, Immunolocalization of glucomannans in the cell wall of differentiating tracheids in *Chamaecyparis obtuse*, Protoplasma 213 (2000) 148–156.
[39] T. Deák, T. Kupi, R. Oláh, L. Lakatos, L. Kemény, G.D. Bisztray, E. Szegedi, Candidate plant gene homologues in grapevine involved in *Agrobacterium* transformation, Cent. Eur. J. Biol. 8 (2013) 1001–1009.
[40] J.C. Mortimer, X. Yu, S. Albrecht, F. Sicilia, M. Huichalaf, D. Ampuero, L.V. Michaelson, A.M. Murphy, T. Matsunaga, S. Kurz, E. Stephens, T.C. Baldwin, T. Ishii, J.A. Naiper, A.P.M. Weber, M.G. Handford, P. Dupree, Abnormal glycosphingolipid mannosylation triggers salicylic acid-mediated responses in *Arabidopsis*, Plant Cell 25 (2013) 1881–1894.